

CLEARED
FOR PUBLIC RELEASE
AFRL/DE 77A
27 JUL 05

Theoretical Notes

Note 176

April 1973

Cable Response to System-Generated EMP

K.S.H. Lee

Dikewood Corporation, Westwood Research Branch
Los Angeles, California

Abstract

Curves and approximate formulas are given for the induced open-circuit voltage of a wire near a wall and/or a right-angled corner of an enclosure bombarded externally by X-rays and γ -rays.

AFRL/DE 04-445

I. Introduction

The geometry of the problem considered in this note is depicted in Figure 1a where a wire, bare or insulated, is inside a system (which we will simply call an enclosure) bombarded externally by X-rays and γ -rays. These photons interact with the enclosure walls as well as the wire, thereby creating charged particles within the enclosure and, hence, voltages and currents in the loads connecting the wire and the enclosure wall. This note is concerned with calculating these voltages and currents.

Using the same assumptions that Baum has made in his work [1], [2] we reduce our problem to a static one. Furthermore, we assume that the distance of the wire from the nearest wall is much smaller than the wire's length and our problem is then reduced to a two-dimensional electrostatic boundary-value problem.

In order to calculate the induced voltages and currents in the loads Z_1 and Z_2 (Figure 1a) one needs to know the equivalent height and the characteristic impedance (or capacitance per unit length) of the wire with respect to the wall. The equivalent height together with the incident electric field gives the open-circuit voltage, and with the time rate of change of the incident magnetic field it gives the longitudinal impressed voltage on the wire [3]. The incident electric and magnetic fields can be very easily calculated for a large variety of enclosure shapes [1] and will not be done in this note. Instead, we will concentrate on the calculation of the equivalent height and study its dependence on the wire distance from the nearest wall. The concept of equivalent height is useful when the incident fields are almost constant between the wire and the wall. But, when the wire is near a corner or at some distance away from the nearest wall, it is more useful to speak of a quantity called the voltage scaling factor defined as the ratio of the induced open-circuit potential on the wire to the incident potential at the position of the wire. The wire capacitance per unit length within two parallel plates can be obtained quite accurately by adding the wire capacitance with respect to one plate to that with respect to the other plate [4]. When the wire is near a corner a simple image theory of line charges will give a sufficiently accurate formula for the wire capacitance per unit length. In the case where electrical wavelengths of interest are larger than the wire length, the open-circuit voltage is the most important quantity as far as induced voltages and currents in the

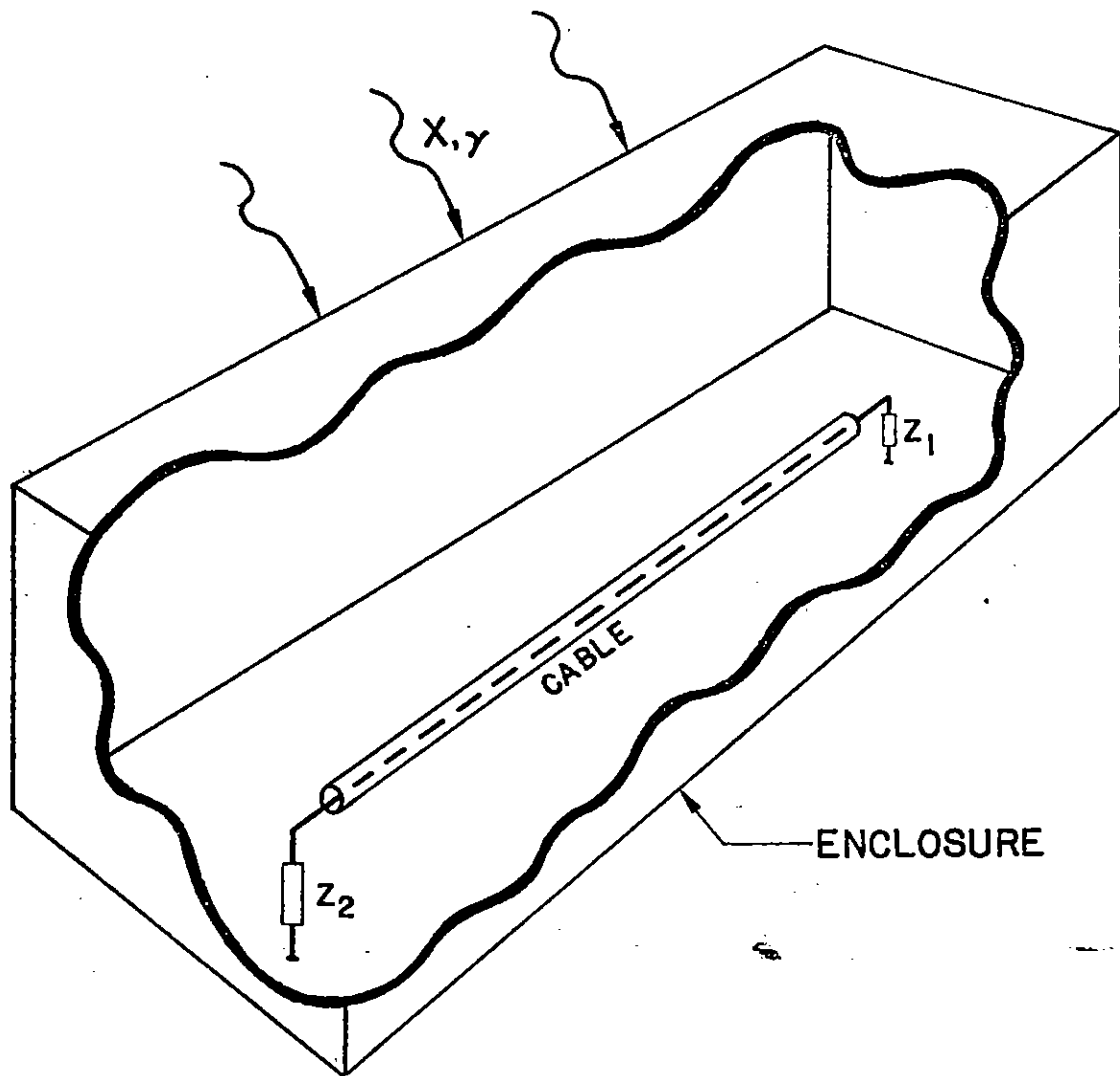


Figure 1a. A bare or insulated wire inside an enclosure bombarded by X-rays and γ -rays.

loads are concerned. Figure 1b shows the equivalent circuit for one representative section of the wire considered in Figure 1a. The various quantities in the figure are defined as follows:

$$C \approx 2\pi\epsilon \left[\frac{1}{\ln \frac{2h}{a}} + \frac{1}{\ln \frac{2(d-h)}{a}} \right], \quad \text{farads/meters}$$

(See figure 2 for definitions of d, h and a.)

$$L = \mu\epsilon/C, \quad \text{henries/meter}$$

$$i_s = -CE \dot{V} \cdot \frac{h_{eq}}{a}, \quad \text{amperes/meter}$$

(h_{eq} is the equivalent height of the wire with respect to the bottom plate.)

$$v = -\dot{\Phi}, \quad \text{volts/meter}$$

(Φ is the magnetic flux linkage per unit length between the wire and the bottom plate.)

$$I_c = \text{Compton current source per meter.}$$

Figure 1c shows the equivalent circuit of the entire wire with terminations when the wire length is electrically short. When the wire's cross section is small and the wire is at some distance away from the plates, the total Compton current source I_c is small compared to the signal current [8]. The present note exclusively deals with the calculation of the open-circuit voltage V in Figure 1c or, equivalently, the short-circuit current i_s in Figure 1b.

In Section II a mathematical formulation is given for the boundary-value problem where the wire is between two parallel plates. Approximate expressions are derived in Section III for the equivalent height and the voltage scaling factor when the wire is only a few wire radii away from the nearest plate. These approximate expressions are compared in Section IV with the "exact" results obtained by numerically solving an integral equation, and from the comparison validity criteria are established for the approximate expressions. In Section V a simple approximate solution is given to the problem of a wire near a corner.

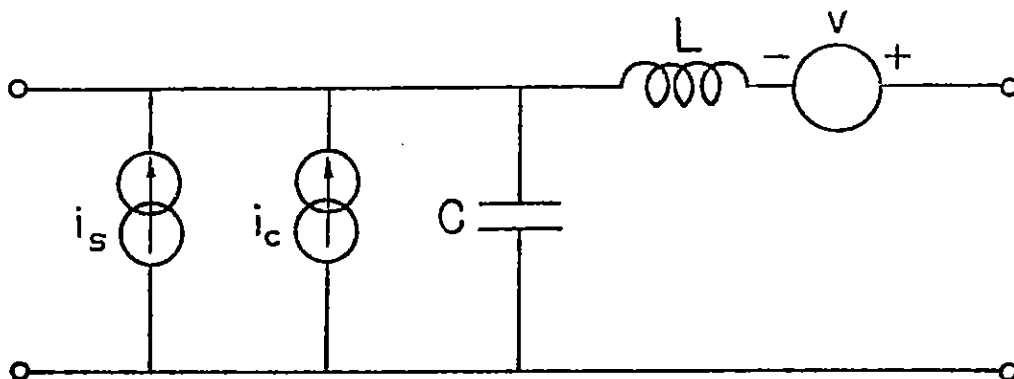


Figure 1b. Equivalent circuit for one section of the wire.

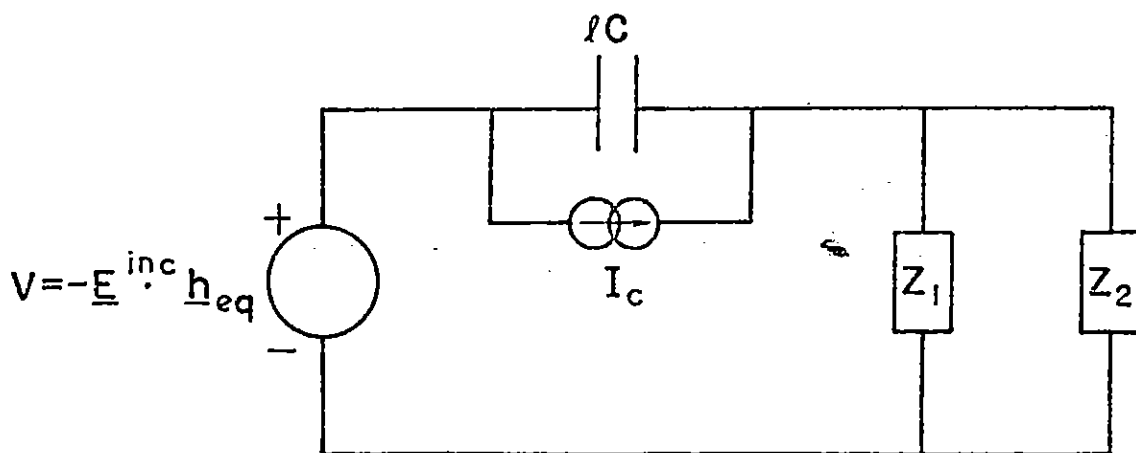


Figure 1c. Equivalent circuit for the terminated wire shown in Figure 1a. (The wire length ℓ is assumed to be electrically short.)

II. Formulation

The problem posed in the Introduction can be stated mathematically as follows. In the region bounded by the wire and the two plates (Figure 2) the potential function ϕ satisfies the Poisson equation

$$\nabla^2 \phi = -\rho/\epsilon \quad (1a)$$

with the boundary conditions

$$\phi = 0, \quad \text{at the plates} \quad (1b)$$

$$\int \frac{\partial \phi}{\partial r_o} a d\theta_o = 0, \quad \text{over the wire's surface} \quad (1c)$$

Here, ρ is the Compton charge density and assumed to be constant in the following analysis, and ϵ is the vacuum permittivity. To solve equations (1) for the induced potential V of the wire it is most expedient to use Green's theorem in which the Green's function G satisfies the following equation

$$\nabla^2 G = -\delta(r_o - r'_o) \frac{\delta(\theta_o - \theta'_o)}{r_o} \quad (2a)$$

with the boundary condition

$$G = 0, \quad \text{at the plates} \quad (2b)$$

Application of Green's theorem to (1) and (2) gives

$$\phi(\underline{r}_o) = \frac{\rho}{\epsilon} \iint_{\underline{A}} G(\underline{r}_o, \underline{r}'_o) r'_o dr'_o d\theta'_o + a \int_0^{2\pi} \phi(a, \theta'_o) \frac{\partial G}{\partial r'_o} d\theta'_o - a \int_0^{2\pi} \frac{\partial \phi}{\partial r'_o} G d\theta'_o \quad (3)$$

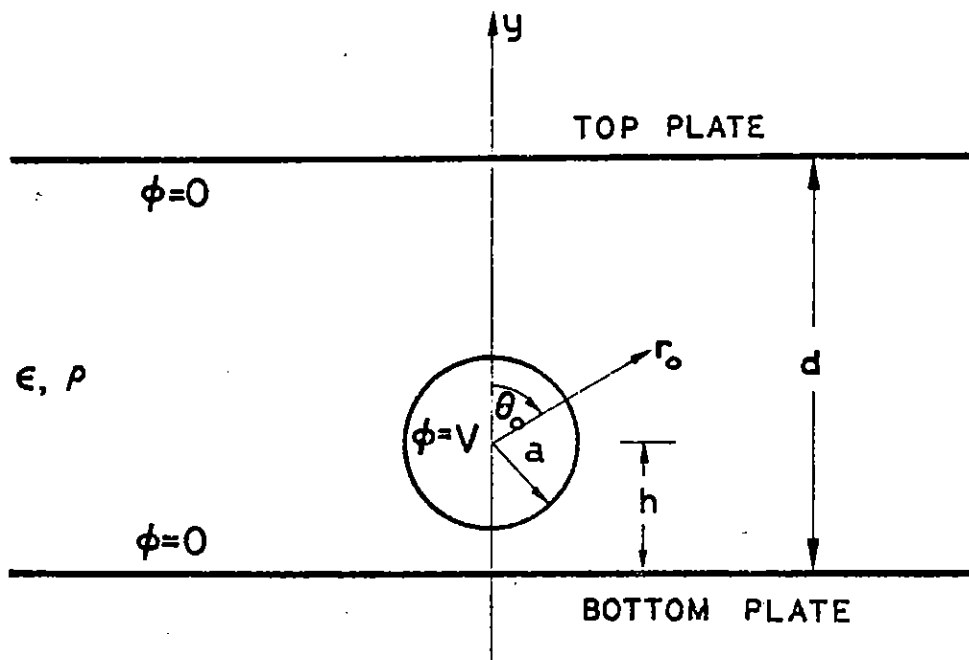


Figure 2. Cross-sectional view of a cylindrical wire inside two parallel plates filled with Compton charge density ρ .

where the observation point \underline{r}_o is not on the cylinder's surface and \bar{A} is the cross-sectional area between the two plates and the cable. Since ϕ is constant on the wire, equation (3) is reduced to

$$\phi(\underline{r}_o) = \frac{\rho}{\epsilon} \iint_{\bar{A}} G(\underline{r}_o, \underline{r}'_o) r'_o dr'_o d\theta'_o - a \int_0^{2\pi} \frac{\partial \phi}{\partial r'_o} G d\theta'_o \quad (4)$$

There are a few representations for the Green's function G which satisfies equations (2). The most suitable representation, from both the mathematical and physical viewpoint, is obtained from the image theory. One can easily find that

$$G = \sum_{m=-\infty}^{\infty} (-)^m \frac{1}{2\pi} \ln \frac{1}{|\underline{r}_m - \underline{r}'_m|} \quad (5)$$

where \underline{r}_m and \underline{r}'_m are shown in Figure 3 and

$$|\underline{r}_m - \underline{r}'_m| = [r_m^2 + r_m'^2 - 2r_m r_m' \cos(\theta_m - \theta'_m)]^{1/2} \quad (6)$$

One can expand the logarithmic function in (5) in an infinite series and obtains [4]

$$G = \sum_{m=-\infty}^{\infty} (-)^m \left[\frac{1}{2\pi} \sum_{n=1}^{\infty} \frac{1}{n} \left(\frac{r'_m}{r_m} \right)^n \cos n(\theta_m - \theta'_m) - \frac{\ln r_m}{2\pi} \right], \quad r_m > r'_m \quad (7)$$

Let us now examine the source term in (3) and denote it by ϕ^s .

$$\begin{aligned} \phi^s(\underline{r}_o) &= \frac{\rho}{\epsilon} \iint_{\bar{A}} G(\underline{r}_o, \underline{r}'_o) r'_o dr'_o d\theta'_o \\ &= \frac{\rho}{\epsilon} \iint_P G r'_o dr'_o d\theta'_o - \frac{\rho}{\epsilon} \iint_C G r'_o dr'_o d\theta'_o \\ &= \phi^P(\underline{r}_o) - \phi^C(\underline{r}_o) \end{aligned} \quad (8)$$

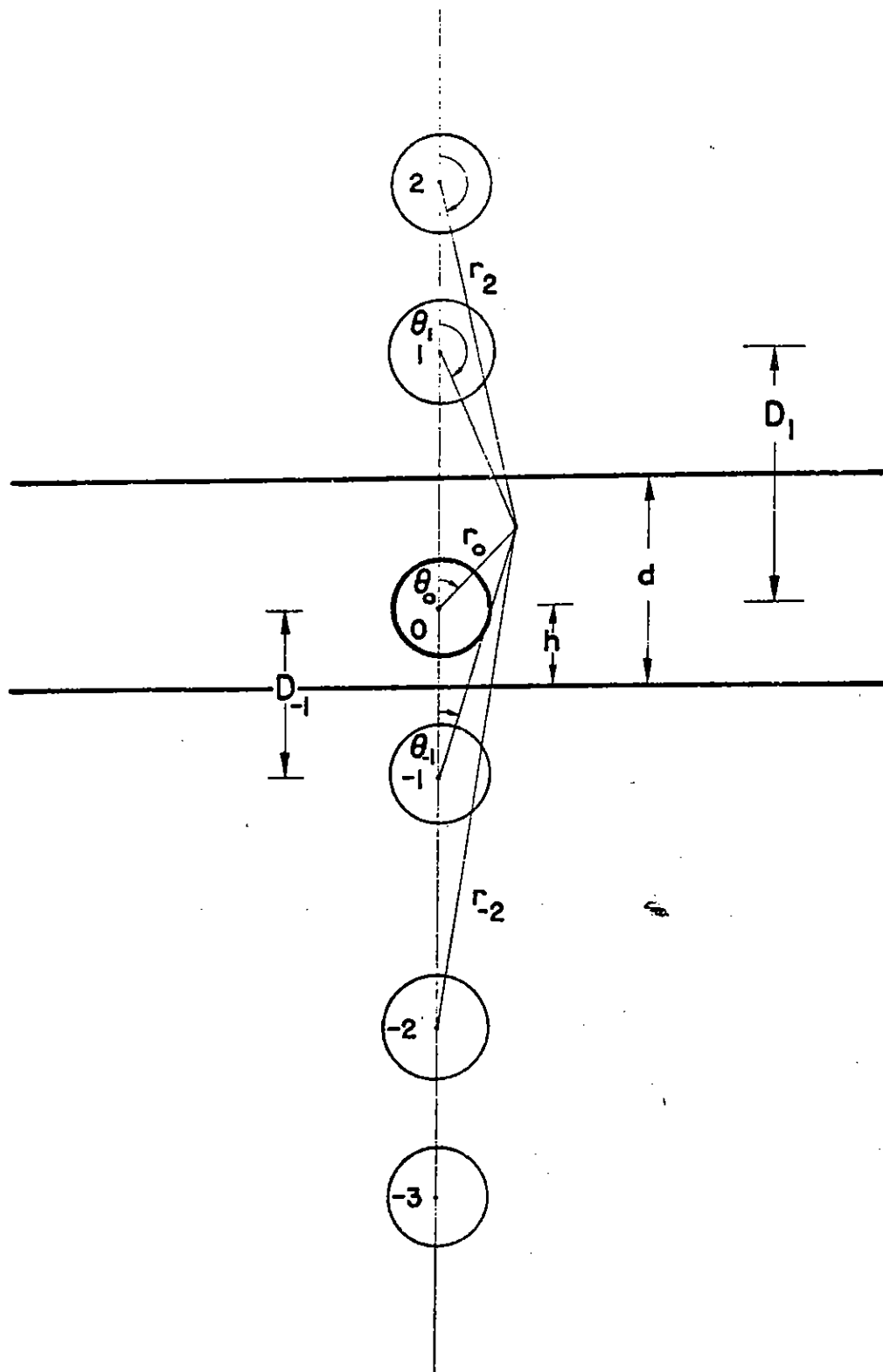


Figure 3. The coordinates of the primary circle 0 and its images.

where P denotes the entire area between two plates, and C the area of the circle. By solving Poisson's equation between two plates or by a direct integration one has

$$\phi^P(\underline{r}_0) = \frac{\rho}{2\epsilon} (h + r_0 \cos \theta_0)(d - h - r_0 \cos \theta_0) \quad (9)$$

where h and d are shown in Figure 3. Substituting (7) in ϕ^C and integrating term by term we obtain

$$\phi^C(\underline{r}_0) = \frac{\rho a^2}{2\epsilon} \sum_{m=-\infty}^{\infty} (-)^m \ln\left(\frac{1}{r_m}\right) \quad (10)$$

Note that both ϕ^P and ϕ^C vanish at the plates. Also note that ϕ^P is identical to the result obtained previously [1].

Now we let

$$\sigma_0 = -\epsilon \frac{\partial \phi}{\partial r_0} \quad (11)$$

and expand

$$\sigma_0 = \sum_{k=1}^{\infty} s_k \cos k\theta_0 \quad (12)$$

where we have omitted the $k = 0$ term to ensure the total induced charges on the cylinder to be zero in accord with the boundary condition (1c). We also observe that the following is true [5], [6]:

$$\sigma_m(\theta_m) = \sigma_0(\theta_m), \quad \text{for } m \text{ even} \quad (13)$$

$$\sigma_m(\theta_m) = -\sigma_0(\pi - \theta_m), \quad \text{for } m \text{ odd}$$

[see Figure 3], where σ_m is the charge density on the m -th image cylinder.

Using (7), (11), (12) and (13) in (4) and letting the observation point \underline{r}_0 lie on the primary cylinder we obtain

$$V = \phi^S(\theta_0) + \frac{a}{2\epsilon} \sum_{m=-\infty}^{\infty} \sum_{n=1}^{\infty} \epsilon_{mn} \frac{s_n}{n} \left(\frac{a}{r_m}\right)^n \cos n\theta_m \quad (14)$$

where $\epsilon_{mn} = 1$ for even m and $\epsilon_{mn} = (-1)^{m+n}$ for odd m . Equation (14) is similar to those derived in references [5] and [6]. In a later section we will start from (14) and generate a matrix equation for s_n from which we determine the induced voltage V . In this respect our method is different from that used in [5] and [6] where the "extended boundary condition" of Smythe [7] has been used.

III. Approximate Solutions

In most practical applications the wire radius a is much less than the plate spacing d , and the distance h of the wire from the nearest plate is about a few wire radii (see Figure 2). In this section we will obtain for this case some approximate solutions for the wire potential V accurate up to order $(a/d)^2$. In the next section we will numerically solve (14) for V .

We begin with (14) and expand that equation in a cosine series. By comparing coefficients in this series expansion we obtain the matrix equation

$$\sum_{k=0}^{\infty} A_{jk} x_k = c_j, \quad j = 0, 1, 2, \dots \quad (15)$$

where

$$A_{jk} = \left(\frac{5\delta_{oj} - 1}{2} \right) \delta_{jk} - (1 - \delta_{ok}) M_{jk} \quad (16)$$

$$c_j = 2 \left(\frac{2\epsilon}{\rho d^2} \right) \frac{1}{2\pi} \int_0^{2\pi} \phi^s(\theta_o) \cos j\theta_o d\theta_o \quad (17)$$

$$x_o = \left(\frac{2\epsilon}{\rho d^2} \right) V \quad (18)$$

$$x_j = \frac{2as_j}{\rho d^2 j}, \quad j = 1, 2, 3, \dots \quad (19)$$

and M_{jk} is given in Appendix A.

Let us now proceed to the calculation of the source term c_j defined by (17). According to (8), (9) and (10) we have

$$\frac{2\epsilon}{\rho} \phi^s(\theta_o) = (h + a \cos \theta_o)(d - h - a \cos \theta_o) - a^2 \sum_{m=-\infty}^{\infty} (-)^m \ln \left(\frac{1}{r_m} \right) \quad (20)$$

where

$$r_m = [D_m^2 + a^2 + 2aD_m \cos \theta_o]^{1/2}, \quad m \neq 0$$

$$r_o = a$$

and D_m is the distance between the centers of the 0-th and m-th circle. Inspection of Figure 3 shows that

$$D_{2m} = 2|m|d, \quad m = \pm 1, \pm 2, \dots \quad (21)$$

$$D_{2m-1} = |2md - 2h|, \quad m = 0, \pm 1, \pm 2, \dots$$

Also, it is quite easy to establish that

$$\frac{1}{2\pi} \int_0^{2\pi} \ln \frac{1}{r_m} d\theta_o = \ln \frac{1}{D_m}, \quad m \neq 0 \quad (22)$$

$$\ln \frac{1}{a} + \sum_{m \neq 0} (-)^m \ln \frac{1}{D_m} = \ln \left[\frac{2h \cdot \sin(\pi h/d)}{a \cdot \pi h/d} \right]$$

Using (20)-(22) in (17) we obtain

$$c_o = 2\beta(1 - \beta) - \alpha^2 \left[1 + 2 \ln \frac{2 \sin \pi\beta}{\pi\alpha} \right] \quad (23)$$

$$c_j = \alpha(1 - 2\beta)\delta_{1j} - \frac{\alpha^2}{2} \delta_{2j}$$

$$+ (-)^{j+1} \frac{\alpha^2}{j} \left[1 - \left(\frac{\alpha}{2\beta}\right)^j + \left(\frac{\alpha}{2}\right)^j \sum_{m=1}^{\infty} \frac{2(1-\beta^2/m^2)^j - (1-\beta/m)^j - (1+\beta/m)^j}{m^j (1-\beta^2/m^2)^j} \right], \quad j \neq 0$$

where $\alpha = a/d$ and $\beta = h/d$.

We now solve (15) for V approximately, assuming that $\alpha \ll 1$ and β is greater than a few α 's. The first approximation gives

$$x_o^{(1)} = c_o/2 = \beta(1 - \beta) - \alpha^2 \left[\frac{1}{2} + \ln\left(\frac{2 \sin \pi\beta}{\pi\alpha}\right) \right] \quad (24)$$

where x_o is related to V by (18). The square bracketed term exists because of the presence of the wire. From (14) it is clear that if the contributions from all the multipoles can be neglected, the average value of ϕ^s over the wire's surface is the open-circuit voltage, V , induced on the wire.

To obtain the second approximation we take the matrix in (15) to be 2×2 . Neglecting terms higher than α^2 we obtain

$$x_o^{(2)} = x_o^{(1)} - \pi\alpha^2(1/2 - \beta)\cot(\pi\beta) \quad (25)$$

Expressions (24) and (25) are even functions of β about $\beta = 1/2$, i.e., the mid-plane between the two plates. Thus, one needs only to consider them for $1/2 \geq \beta > \alpha$. (The case $\beta = \alpha$ means that the wire touches the bottom plate.) Usually, α is very small and hence the term proportional to α^2 in (24) and (25) is negligible for almost all β except when β is comparable to α . When β is equal to a few α 's, (25) takes the approximate form

$$x_o^{(2)} \approx \beta - \frac{\alpha^2}{2\beta} \quad (26)$$

Let us introduce the equivalent height, h_{eq} , defined by

$$h_{eq} \equiv \frac{V}{E^{inc}} = x_o d \quad (27)$$

where E^{inc} is electric field evaluated at the bottom plate (Figure 2) with

the wire being absent. Then, from (26) and (9) we have

$$\frac{h_{eq}}{a} \approx \frac{h}{a} - \frac{1}{2(h/a)} \quad (28)$$

Let us also introduce the voltage scaling factor, f_v , defined by

$$f_v \equiv \frac{V}{\phi^{inc}} = \frac{x_0}{\beta(1-\beta)} \quad (29)$$

where ϕ^{inc} is the incident potential at the position of the wire when the wire is absent. Then, from (26) and (9) we have

$$f_v \approx 1 - \frac{1}{2(h/a)^2} \quad (30)$$

The approximate equations (28) and (30) are shown in Figures 8 and 9 together with the exact results.

The approximate expressions (24) and (25) are plotted in Figures 4-7 together with the exact results for the case where $\alpha = 0.1$ and 0.01 . For thinner wires, i.e., $\alpha < 10^{-2}$, these expressions agree more closely with the exact answer.

In order to use the curves for h_{eq} and f_v in Figures 4-9 to estimate the induced voltage V let us use some typical numbers to express ϕ^{inc} and E^{inc} in terms of the incident gamma flux [1]. Using the numbers in [1] we get

$$\begin{aligned} \phi^{inc} &= \phi^p \approx 10^{-5} \gamma h(d-h)/2 \quad \text{volts} \\ &\approx 10^{-5} \gamma (hd/2) \quad \text{volts} \quad \text{(when close to the bottom plate)} \\ E^{inc} &\approx 10^{-5} \gamma d/2 \quad \text{volts/meters} \quad \text{(at the bottom plate)} \end{aligned}$$

where γ is in roentgens/sec and h and d are in meters. Thus,

$$V \approx 10^{-5} \gamma [h(d-h)/2] f_v \quad \text{volts}$$

or

$$V \approx 10^{-5} \gamma (dh_{eq}/2) \quad \text{volts}$$

Of course, when the wire is very close to the bottom plate, i.e., $d \gg h$, we have $hf_v \approx h_{eq}$, as is evident from (28) and (30).

IV. Numerical Solutions

In the preceding section we have obtained certain approximate solutions for the open-circuit voltage V . In this section we will get accurate numerical results for V . The basic equations that will be used for numerical computation are given by (15), (16) and (23).

The matrix equation (15) was solved for α ranging from 10^{-1} to 10^{-4} and for β ranging from 1.5α to 0.5 . It was found that in the worst case where $\alpha = 0.1$ and $\beta = 1.5\alpha$, a 10×10 matrix gave accuracy to four-significant figures.

In Figure 4 (where $\alpha = 0.1$) and in Figure 5 (where $\alpha = 0.01$) we compare various approximate formulas given by (24), (25) and (28) with equation (15) for the normalized equivalent height defined by (27) as

$$\frac{h_{eq}}{a} = \frac{x_0}{\alpha}$$

For $\alpha \leq 10^{-2}$ and β equal to a few α 's (i.e., the wire is only a few wire radii from the wall) the simple approximate formula (28) is accurate within 5% for $2\alpha \leq \beta \leq 10\alpha$.

In Figures 6 and 7 we plot various approximate formulas (24), (25) and (30) together with the "exact" one (15) for the voltage scaling factor defined by (29) as

$$f_v = \frac{x_0}{\beta(1-\beta)}$$

For $\alpha \leq 10^{-2}$ the simple approximate formula (30) is larger than the "exact" result by not more than 6% for $\beta \geq 1.5\alpha$, and 2% for $\beta \geq 2\alpha$.

In most practical cases the wire is at a distance h of only a few wire radii a away from the wall. In order to show the fine details we plot h_{eq}/a against h/a in Figure 8 with the normalized wire radius α ($\alpha = a/d$) as a parameter. In Figure 9, f_v is graphed against h/a with α as a parameter. We show, in Figure 10, the voltage scaling factor f_v over the entire range, i.e., from the bottom wall to the mid-plane of the two walls.

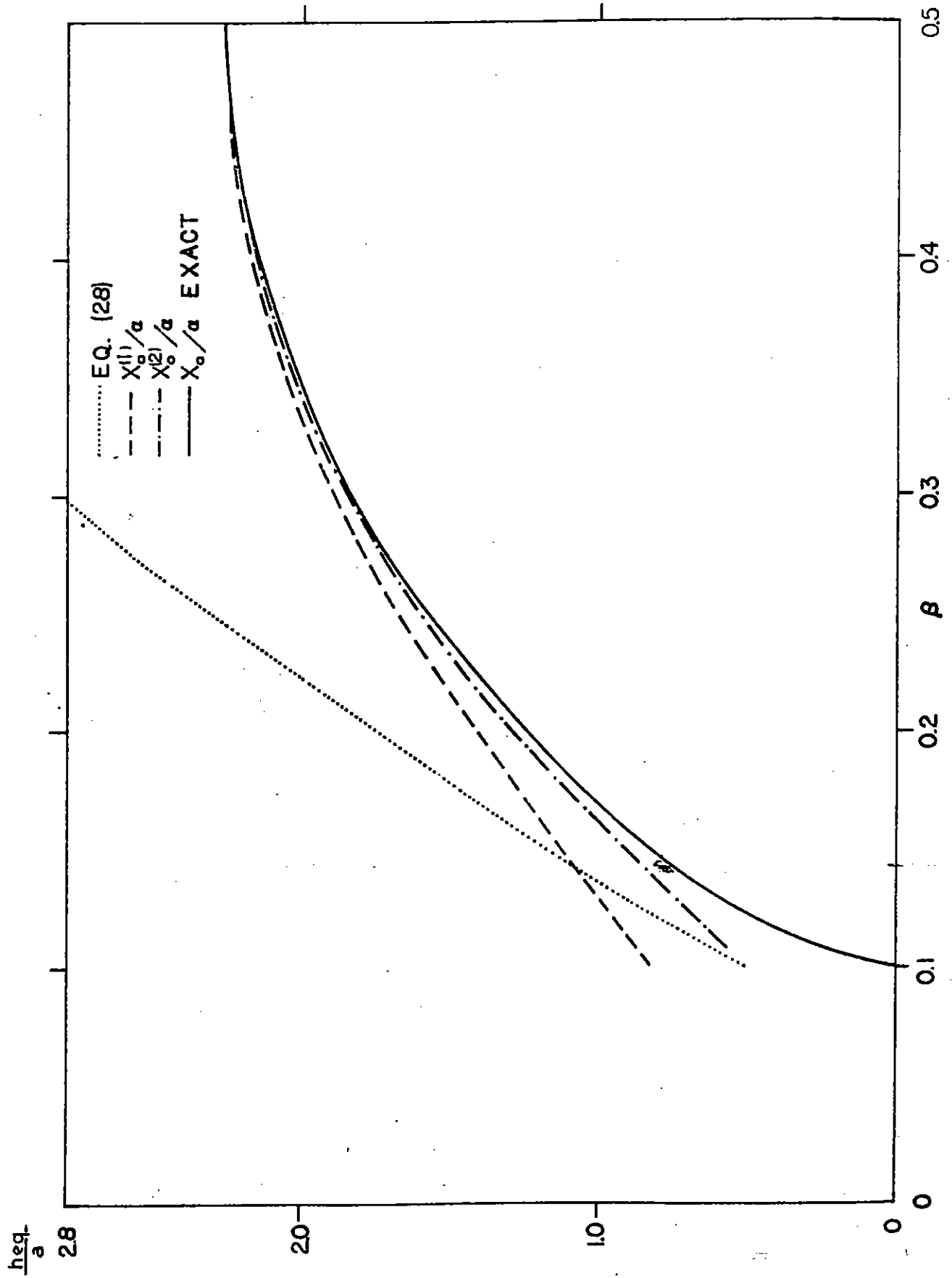


Figure 4. Various approximate formulas for the normalized equivalent height at $\alpha = 0.1$.

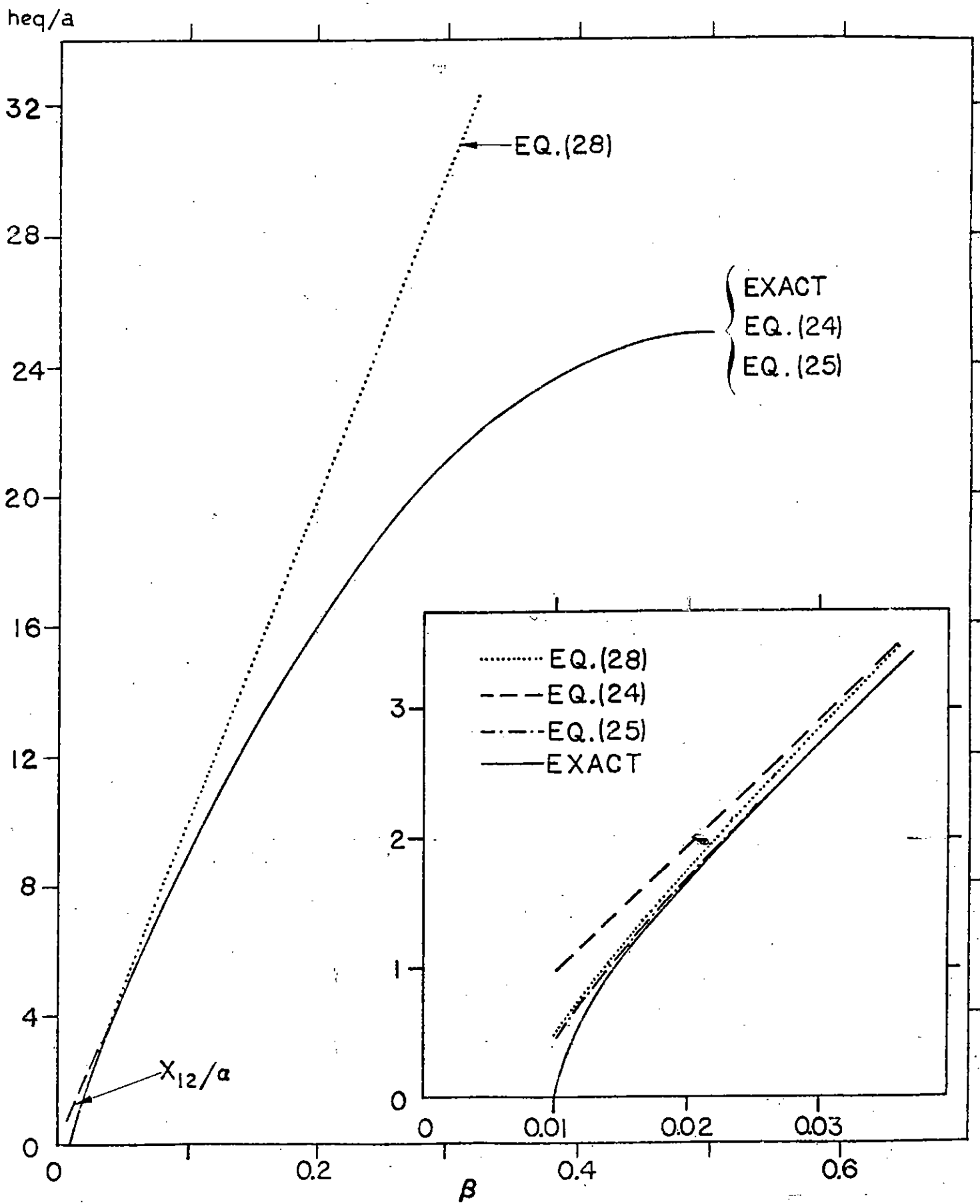


Figure 5. Various approximate formulas for normalized equivalent height at $\alpha = 10^{-2}$.

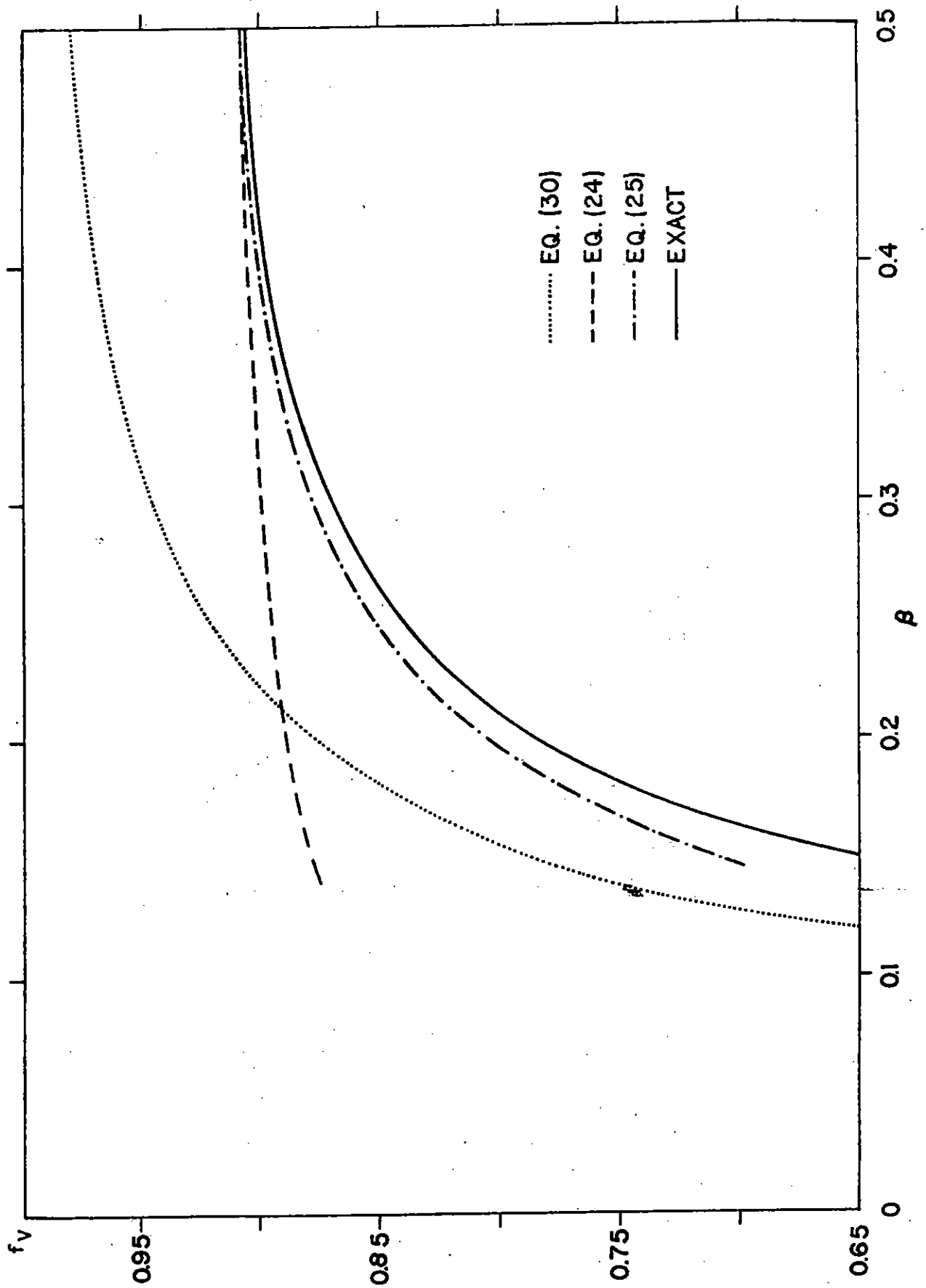


FIGURE 6 Various approximate formulae for the voltage scaling factor at $\alpha = 0.1$

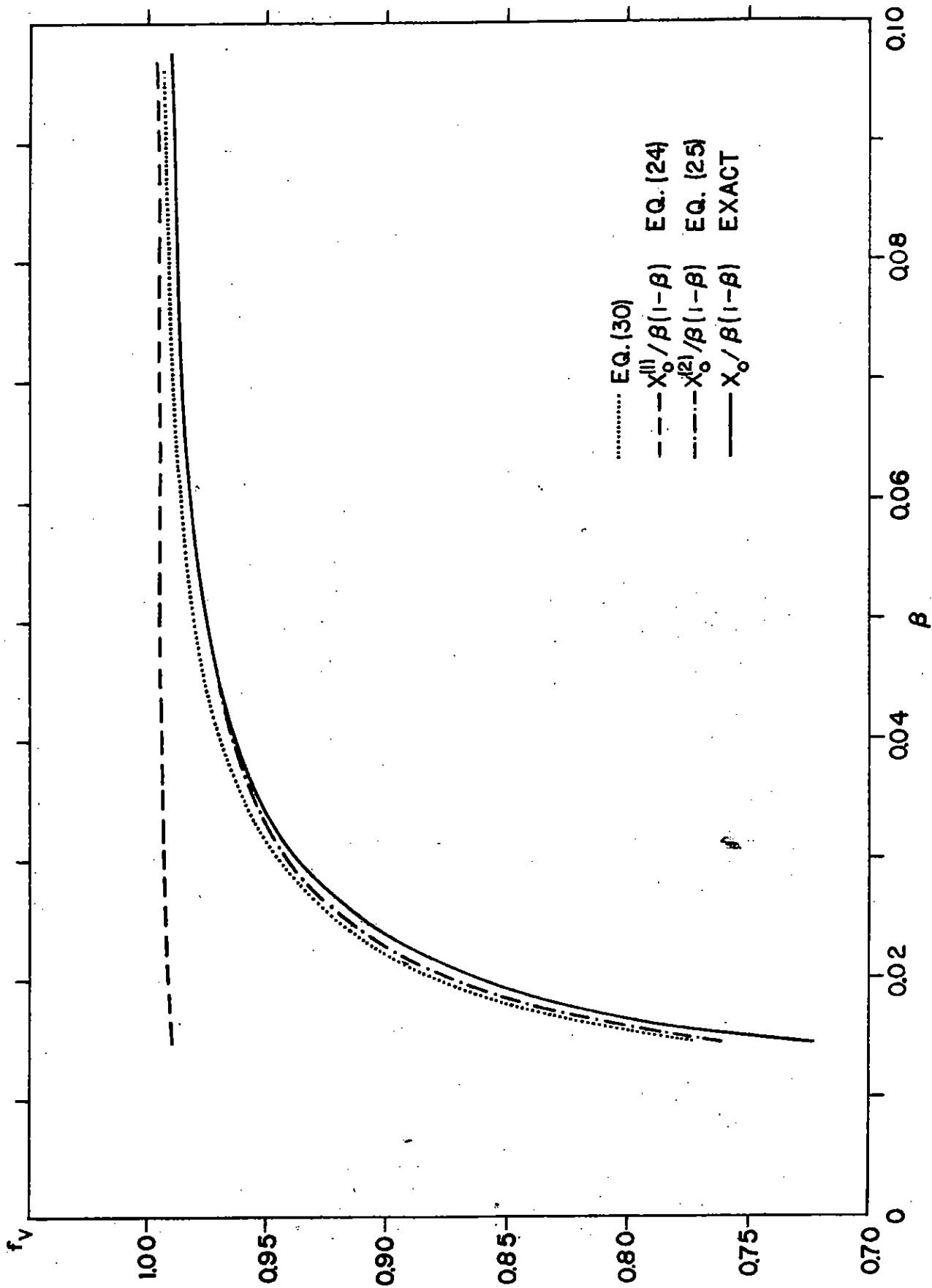


Figure 7. Various approximate formulas for the voltage scaling factor at $\alpha = 10^{-2}$.

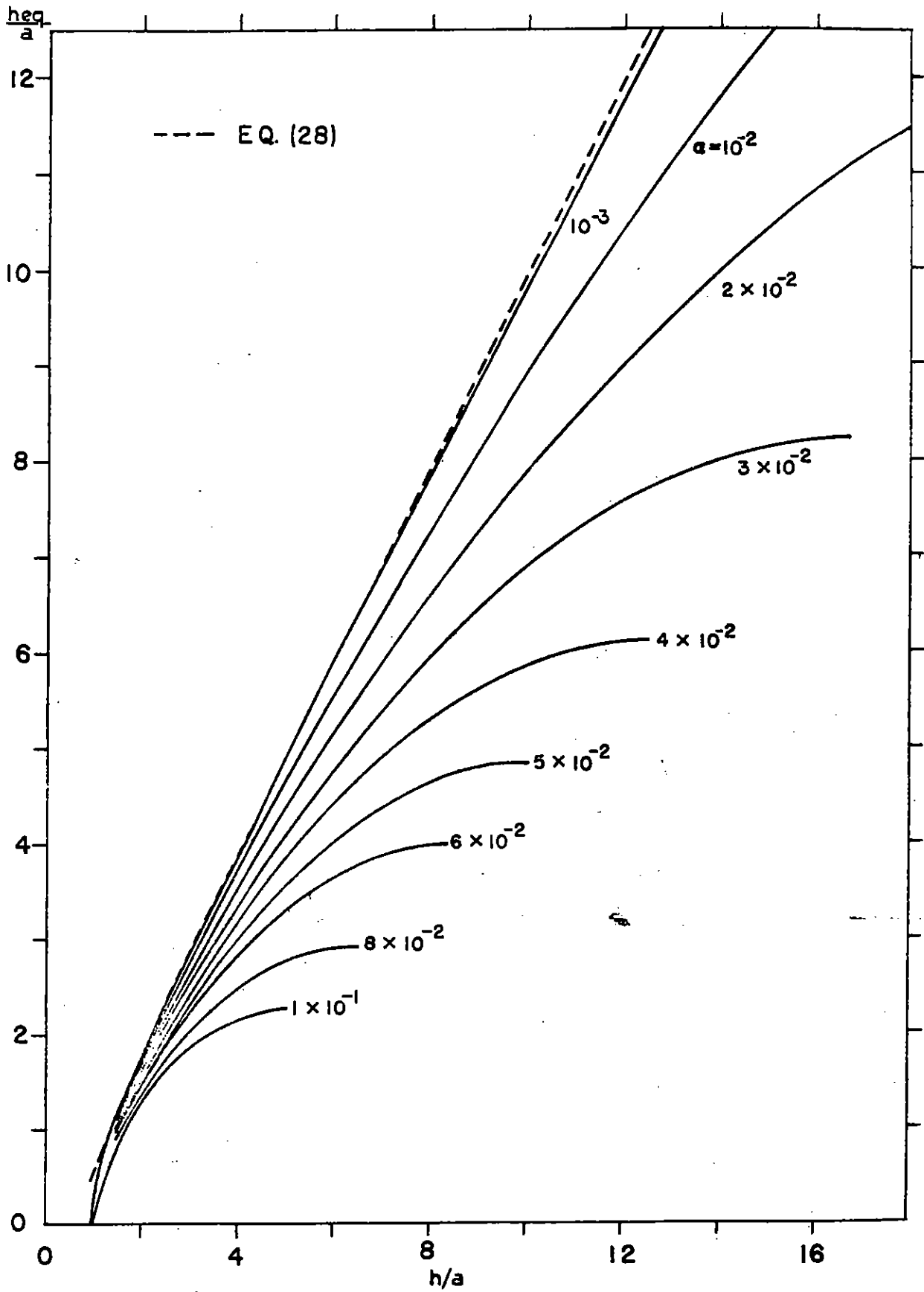


Figure 8. Normalized equivalent height vs. normalized distance from the wall.

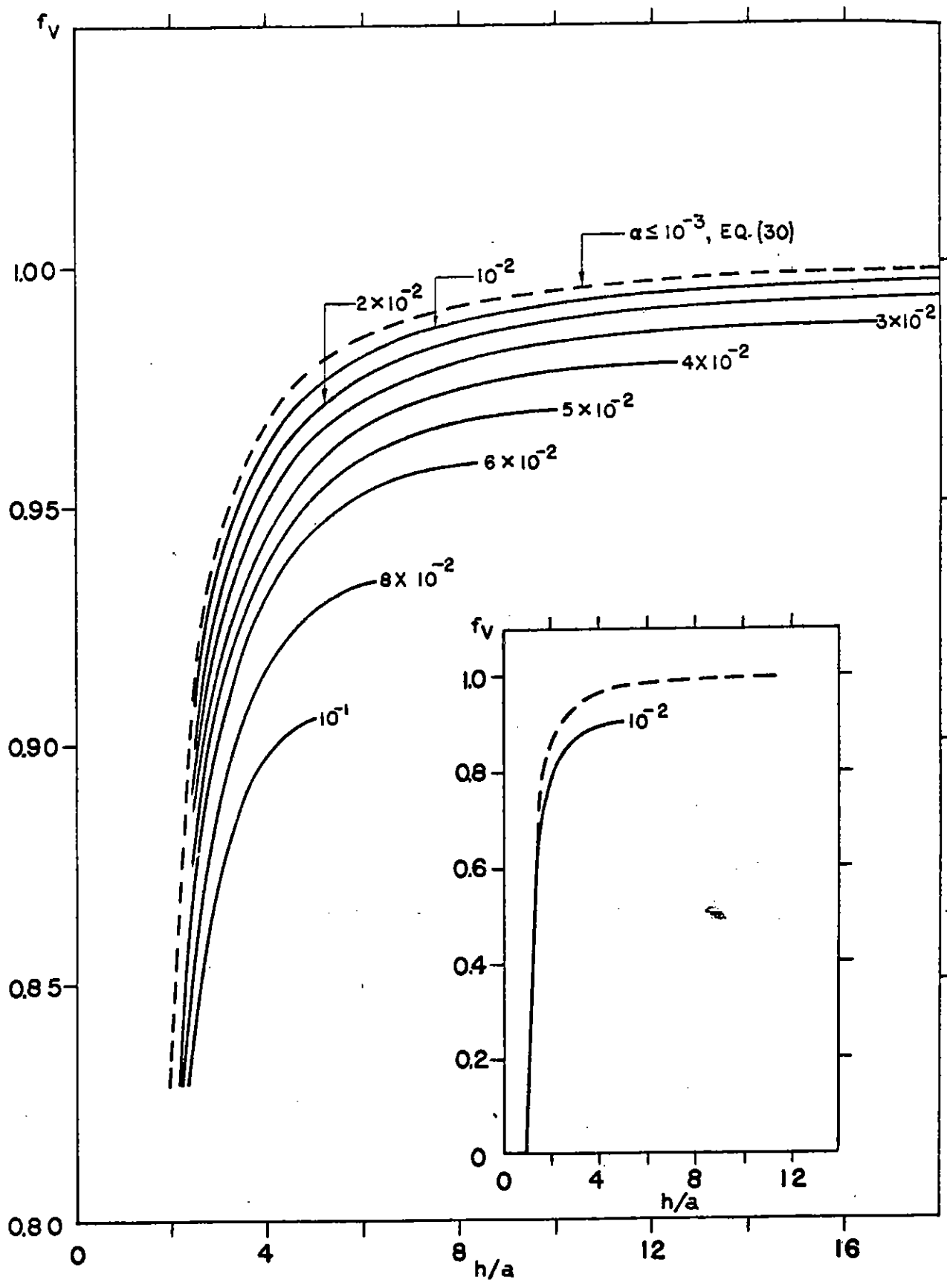


Figure 9. Voltage scaling factor vs. normalized distance from the wall.

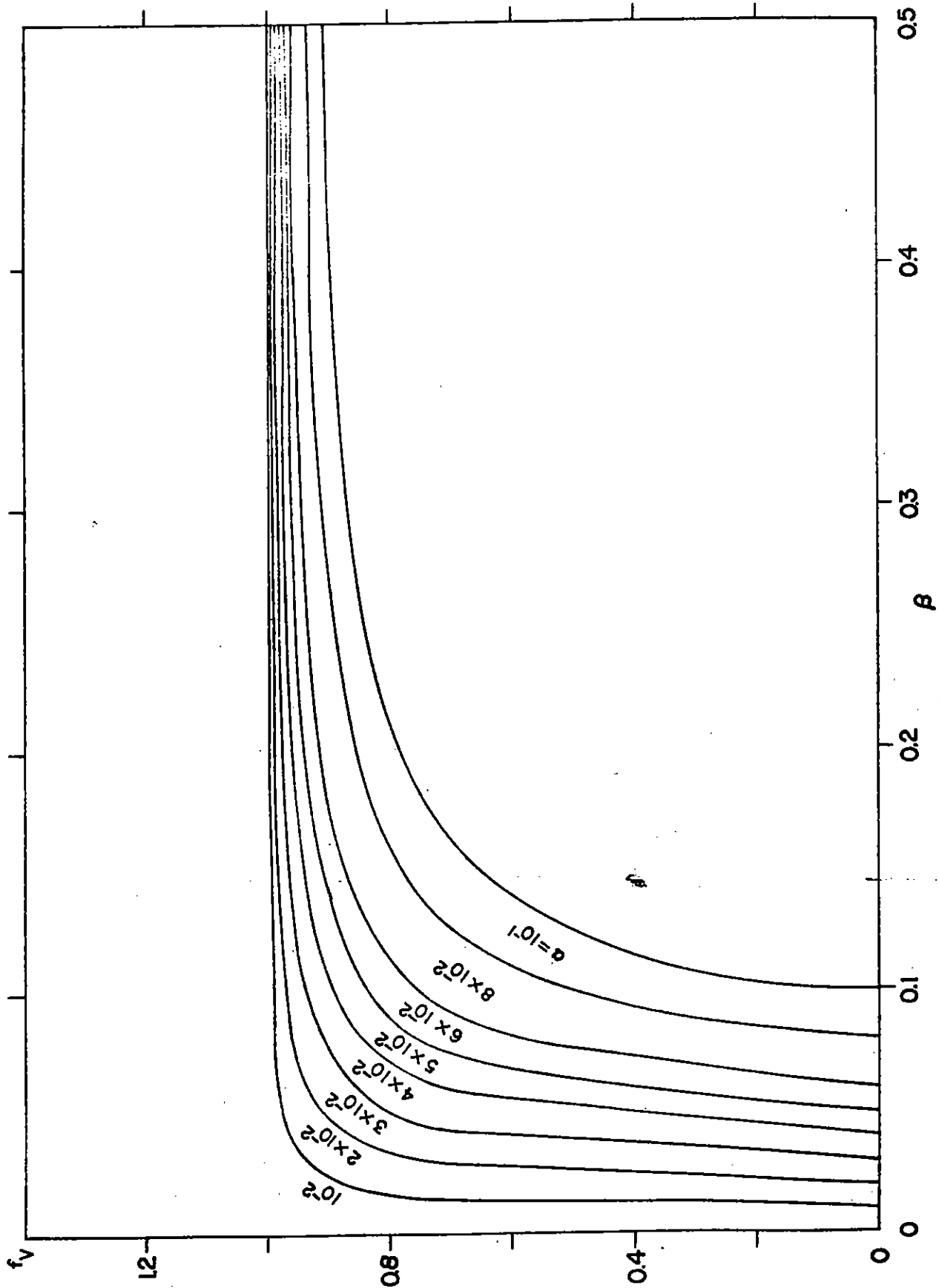


Figure 10. Voltage scaling factor over the entire range.

V. An Isolated Wire Near a Corner

In the preceding section we saw that the simple approximate expression (26) is very accurate when the wire is only a few wire radii away from the wall and when the wire is thin enough. In this section we will give an analogous expression for a thin wire near a right-angled corner of an enclosure. The geometry is depicted in Figure 11. If one follows the procedures that lead to equation (26) it is not too difficult to show that

$$f_v = \frac{V}{\phi_{inc}} \approx 1 - \left(\frac{a}{r}\right)^2 [2 \csc^2(2\theta) - 1] \quad (31)$$

where ϕ^{inc} is the incident potential at the position of the wire when the wire is absent. The usefulness of the quantity of equivalent height in the present case is questionable and calculation for that quantity is therefore omitted. Notice that f_v is symmetric about $\theta = 45^\circ$, as it should. Equation (31) should be accurate within 2% or so if a/c and a/d are not larger than 10^{-2} and if the wire is located within the shaded area as shown in Figure 12. Equation (31) is so simple that one can easily see the r -dependence of f_v . The θ -dependence of f_v is plotted in Figure 13 at various distances from the corner.

Referring to Figure 12 we can rewrite (31) as

$$f_v = 1 - \left[\frac{X^2 + Y^2}{2XY^2} - \frac{1}{X^2 + Y^2} \right] \quad (32)$$

where $X = x/a$ and $Y = y/a$. When either X or Y becomes large, equation (32) reduces to equation (30) which applies to the case of two parallel plates. In Figure 14 we plot equation (32) against y/a at different x/a values. The role of X and Y in these curves can of course be interchanged. We also show equation (30) by dashes and dots. The dashed lines should be used for comparison when $Y > X$, whereas the dotted lines should be used when $Y < X$. By comparing these curves one can get a good feel for the corner's effect on f_v .

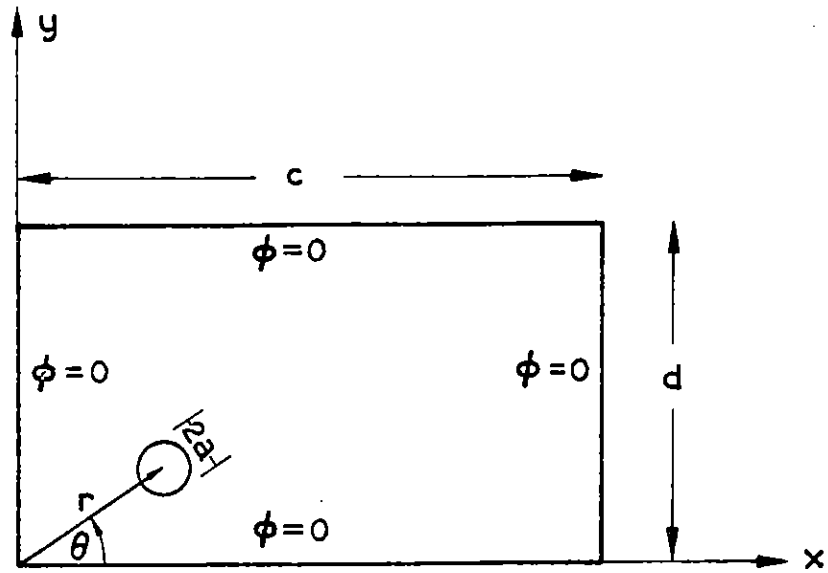


Figure 11. Cross-sectional view of an isolated wire near a corner.

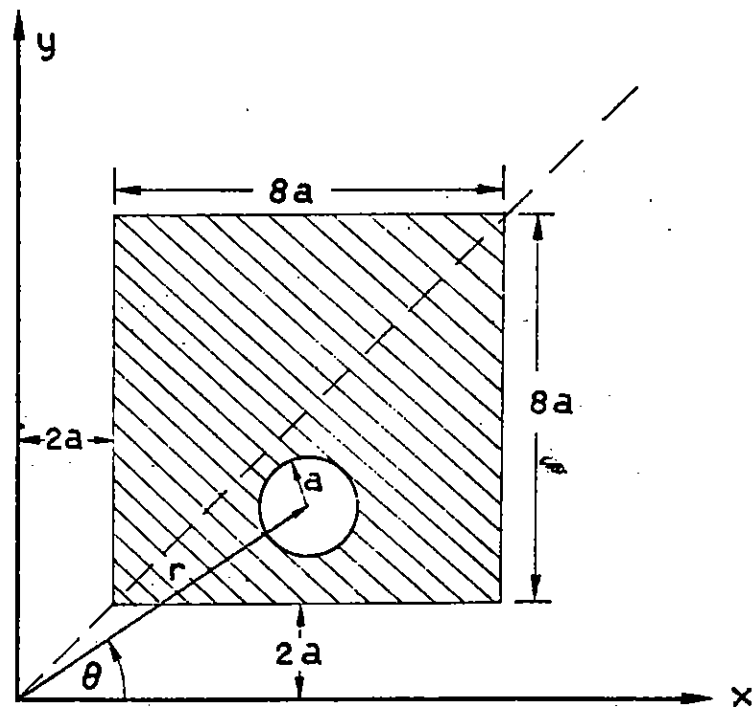


Figure 12. Region of interest is shown as shaded.

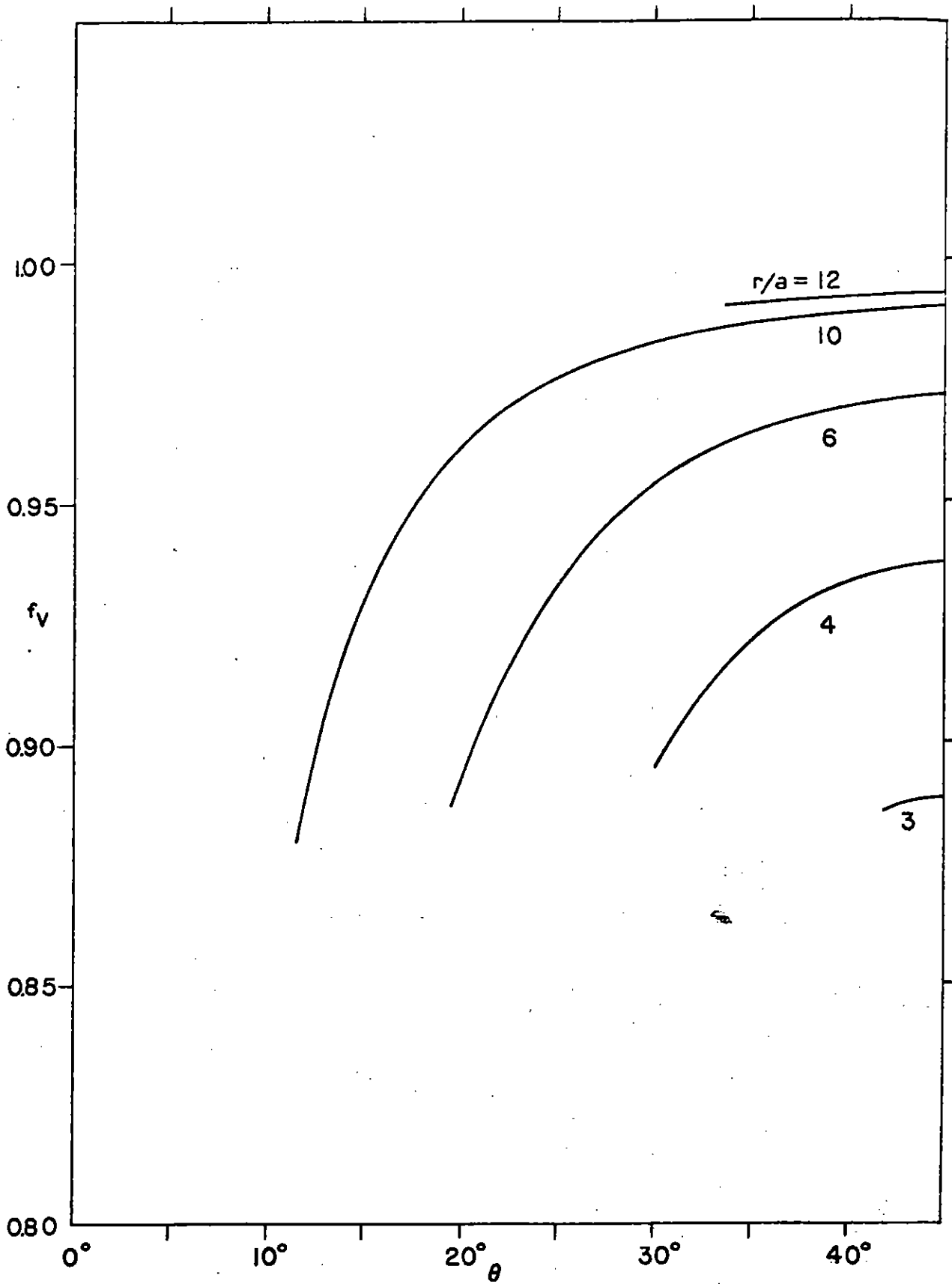


Figure 13. Voltage scaling factor near a corner..

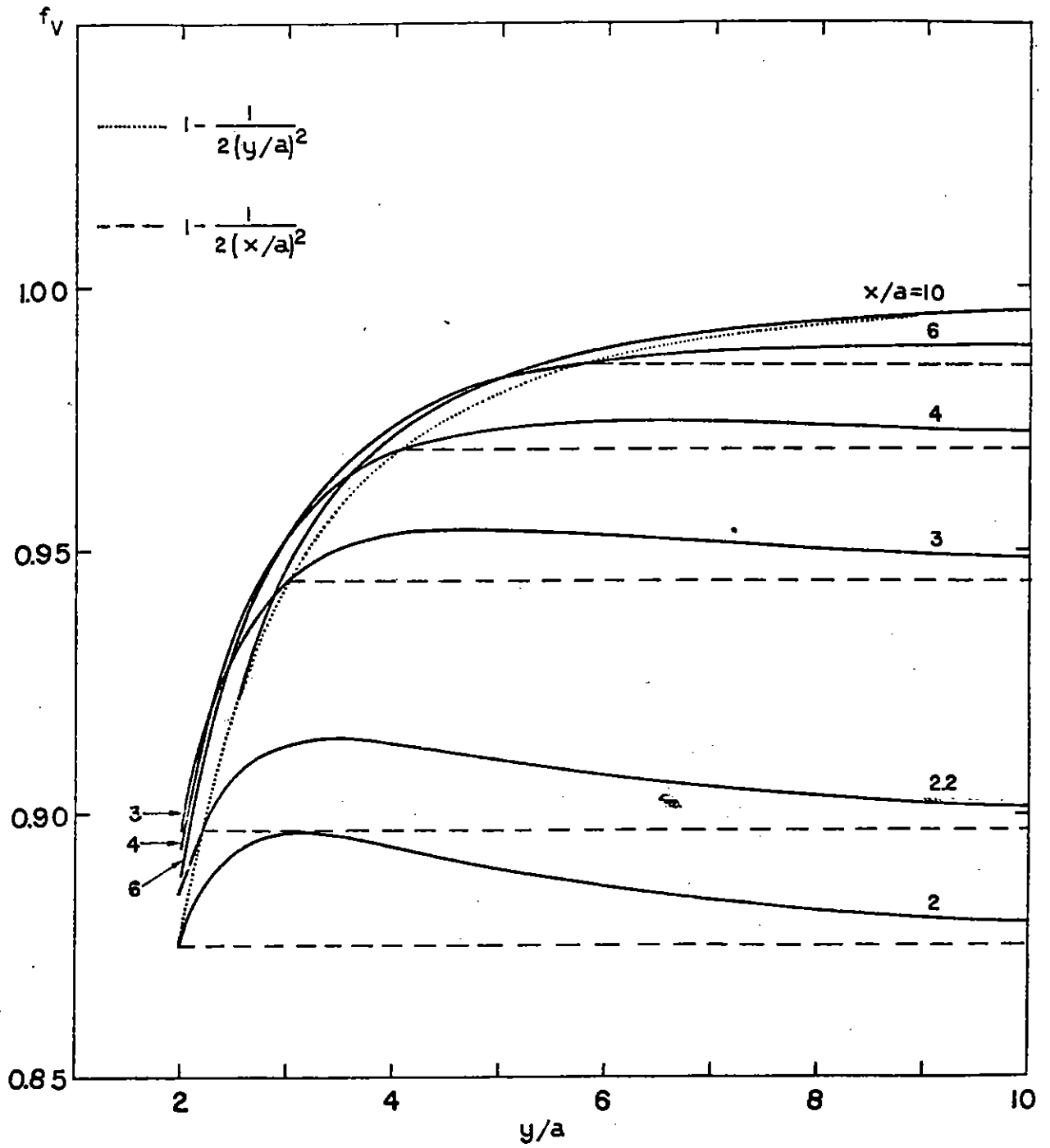


Figure 14. Voltage scaling factor near a corner.

Appendix A

The integrals that appear in the matrix elements M_{jk} are of the form

$$\begin{aligned} I_{jk,m} &= \frac{1}{2\pi} \int_0^{2\pi} \left(\frac{a}{r_m}\right)^k \cos j\theta_0 \cos k\theta_m d\theta_0 \\ &= \frac{a^k}{2} \frac{1}{2\pi} \operatorname{Re} \int_0^{2\pi} \frac{(e^{ij\theta_0} + e^{-ij\theta_0}) e^{-ik\theta_m}}{r_m^k} d\theta_0 \end{aligned}$$

Here, Re denotes the real part of the quantity that follows it. Introducing the complex variable $z = ae^{i\theta_0}$ and noting that $r_m e^{i\theta_m} = z + D_m$ when D_m is on the negative x-axis and $r_m e^{i(\pi-\theta_m)} = D_m - z$ when D_m is on the positive x-axis (see Fig. A) we have

$$\begin{aligned} I_{jk,m} &= \frac{a^k}{2} \operatorname{Re} \left[\frac{1}{2\pi i} \frac{1}{a^j} \oint \frac{z^{j-1}}{(z+D_m)^k} d\theta_0 + \frac{a^j}{2\pi i} \oint \frac{z^{-j-1}}{(z+D_m)^k} d\theta_0 \right], & m < 0 \\ &= \frac{1}{2} \left(\frac{a}{D_m}\right)^k \delta_{oj} + \frac{1}{2} (-)^j \frac{(j+k-1)!}{j!(k-1)!} \left(\frac{a}{D_m}\right)^{j+k}, & m < 0 \end{aligned}$$

and

$$I_{jk,m} = \frac{1}{2} (-)^k \left(\frac{a}{D_m}\right)^k \delta_{oj} + \frac{1}{2} (-)^k \frac{(j+k-1)!}{j!(k-1)!} \left(\frac{a}{D_m}\right)^{j+k}, \quad m > 0$$

Using $D_{2m} = 2|m|d$, $D_{2m-1} = 2|md - h|$, $\alpha = a/d$ and $\beta = h/d$ we obtain for the matrix elements M_{jk} the following

$$\begin{aligned}
2M_{jk} &= 2 \sum_{m \neq 0} I_{jk, 2m} + (-)^{k+1} 2 \sum_{m=-\infty}^{\infty} I_{jk, 2m-1} \\
&= \left(\frac{\alpha}{2}\right)^k \delta_{oj} \sum_{m=1}^{\infty} \left[\left(\frac{1}{m^k} - \frac{1}{(m-\beta)^k} \right) + (-)^k \left(\frac{1}{m^k} - \frac{1}{(m+\beta)^k} \right) \right] \\
&\quad + \left(\frac{\alpha}{2}\right)^{j+k} \frac{(j+k-1)!}{j!(k-1)!} \left\{ \sum_{m=1}^{\infty} \frac{(-)^k}{m^{j+k}} [1 + (-)^{j-k}] - \sum_{m=1}^{\infty} \left[\frac{1}{(m-\beta)^{j+k}} + \frac{(-)^{j+k}}{(m+\beta)^{j+k}} \right] \right\} \\
&\quad + (-)^{k+1} \left(\frac{\alpha}{2\beta}\right)^k \left[\delta_{oj} + (-)^j \frac{(j+k-1)!}{j!(k-1)!} \left(\frac{\alpha}{2\beta}\right)^j \right], \quad \begin{array}{l} j = 0, 1, 2, \dots \\ k = 1, 2, 3, \dots \end{array}
\end{aligned}$$

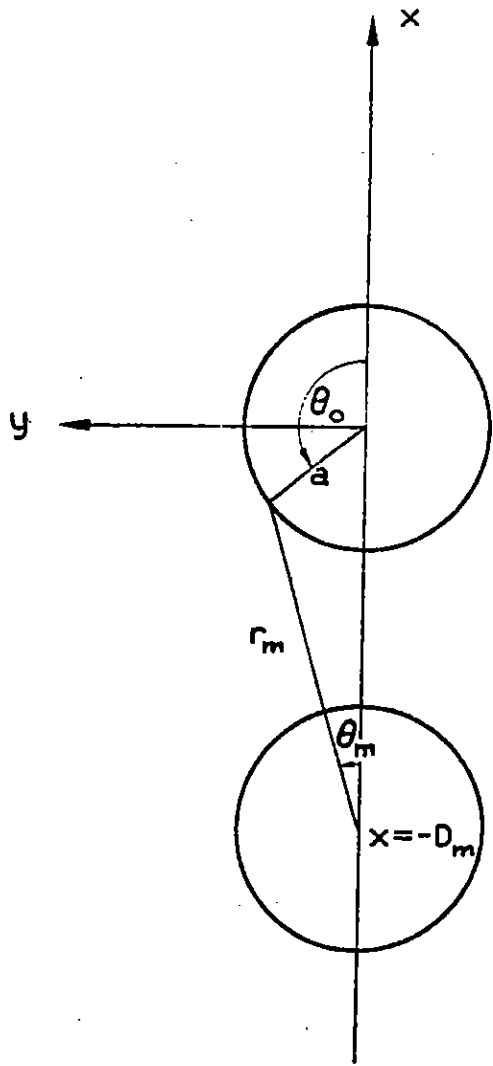


Figure A. The complex z -plane with $z = x + iy$.

Acknowledgment

We had helpful discussions with Dr. Lennart Marin, Dr. Carl Baum, Lt. Larry Williams, and Dr. Phil Castillo. The numerical results were obtained by Dr. Tom Liu.

References

- [1] C. E. Baum, "Unsaturated Compton current and space-charge fields in evacuated cavities," Theoretical Notes, Note 5, January 1965.
- [2] C. E. Baum, "Electrode potentials from Compton current and space charge in evacuated cavities," Theoretical Notes, Note 9, May 1965.
- [3] K. S. H. Lee, "Balanced transmission lines in external fields," Interaction Notes, Note 115, July 1972.
- [4] W. R. Smythe, Static and Dynamic Electricity, 2nd edition, McGraw-Hill, 1950.
- [5] R. W. Latham, "Interaction between a cylindrical test body and a parallel plate simulator," Sensor and Simulation Notes, Note 55, May 1968.
- [6] L. Marin, "Effect of replacing one conducting plate of a parallel-plate transmission line by a grid of rods," Sensor and Simulation Notes, Note 118, October 1970.
- [7] W. R. Smythe, "Charged right circular cylinder," J. Appl. Phys., Vol. 33, No. 10, October 1962.
- [8] C. E. Baum, "A Technique for Measuring Electric Fields Associated with Internal EMP," Sensor and Simulation Notes, Note 24, August 1966.